NUCLEAR THEORY, Vol. 33 (2014)
eds. A.I. Georgieva, N. Minkov, Heron Press, Sofia

Recent Results of the Relativistic Green's Function Model in Quasielastic Neutrino and Antineutrino-Nucleus Scattering

C. Giusti, **A. Meucci**

Dipartimento di Fisica, Università degli Studi di Pavia and
INFN, Sezione di Pavia, via Bassi 6 I-27100 Pavia, Italy

Abstract. The analysis of quasielastic neutrino and antineutrino-nucleus scattering cross sections requires relativistic theoretical descriptions also accounting for the role of final-state interactions (FSI). In the relativistic Green's function (RGF) model FSI are described by a complex optical potential where the imaginary part recovers the contribution of final-state channels that are not included in other models based on the impulse approximation. The RGF results are compared with the data recently published by the MiniBooNE and MINERνA Collaborations. The model is in general able to give a good description of the data.

1 Introduction

Since many years electron scattering has been devised as a powerful and preferential tool to investigate nuclear properties. Several decades of experimental and theoretical work have provided complete and detailed information on nuclear structure and interaction mechanisms [1–3].

Additional information on nuclear properties is in principle available from neutrino-nucleus scattering. The main aim of neutrino experiments, however, is not to study nuclear properties, but to determine neutrino properties. Neutrino physics is of great interest and involves many different phenomena. In neutrino oscillation experiments nuclei are used as neutrino detectors providing relatively large cross sections. Because of the interest in oscillation measurements, various experimental neutrino-nucleus cross sections have been presented [4–11] and are planned in the near future. A proper interpretation of the experimental data requires accurate evaluations of neutrino-nucleus cross sections where all nuclear effects are well under control.

Models developed for electron scattering and tested in comparison with electron scattering data have been applied to describe nuclear effects in neutrino-nucleus scattering. Although different, the two situations present many similar aspects and the extension to neutrino scattering of the electron scattering formalism is straightforward. Moreover, the large amount of detailed experimental information available from electron scattering makes the comparison with electron scattering data the best and most obvious test of the predictive power of a nuclear model.

In this contribution we review recent results obtained with the relativistic Green's function (RGF) model. The model was originally developed, within a nonrelativistic [12, 13] and then a relativistic framework [14, 15], to describe FSI in the inclusive quasielastic (QE) electron scattering, where it has been widely and successfully tested in comparison with data [12, 13, 16–18]. But for some complications due to the Dirac matrix structure, the formalism follows within both frameworks the same steps and approximations. The relativistic version of the model (RGF) has been extended to QE neutrino-nucleus scattering [19–29]. The energy region explored in most neutrino experiments requires a relativistic model, where not only relativistic kinematics is considered, but also nuclear dynamics and current operators are described within a relativistic framework.

2 Final-State Interactions in Quasielatic Lepton-Nucleus Scattering

In the QE kinematic region the nuclear response to an electroweak probe is dominated by one-nucleon processes, where the scattering occurs with only one nucleon, which is then emitted by a direct knockout mechanism, and the remaining nucleons of the target behave as spectators. In electron scattering experiments the emitted nucleon can be detected in coincidence with the scattered electron. Kinematic situations can be envisaged where the residual nucleus is left in a discrete eigenstate and the final state is completely determined. This is the exclusive one-nucleon knockout. The exclusive $(e, e'p)$ reaction has been widely investigated [2]. If only the scattered electron is detected, the final nuclear state is not determined and the measured cross section includes all the available final states. This is the inclusive (e, e') scattering.

Electron and neutrino-nucleus scattering are usually described in the one-boson exchange approximation, where the cross section is obtained from the contraction between the lepton tensor, which essentially depends only on the lepton kinematics, and the hadron tensor $W^{\mu\nu}$, whose components are given by products of the matrix elements of the nuclear current between the initial and final nuclear states. Different models have been developed to calculate the hadron tensor in the exclusive and inclusive processes.

Within the QE kinematic domain, electron scattering can adequately be described by a model based on the nonrelativistic or relativistic impulse approximation (IA or RIA). For the exclusive scattering the IA assumes that the interaction occurs through a one-body current only with a quasi-free nucleon which is then knocked out of the nucleus. For the inclusive scattering, the IA assumes that the cross section is given by the incoherent sum of one-nucleon knockout processes due to the interaction of the probe with all the nucleons of the nucleus. With this assumption, we have the problem to describe the FSI between the emitted nucleon and the residual nucleus.

In the exclusive $(e, e'p)$ reaction FSI are usually described in the distorted-wave impulse approximation (DWIA) by a complex optical potential (OP) where the imaginary part gives an absorption that reduces the calculated cross section. This reduction is essential to reproduce $(e, e'p)$ data. Models based on a non-relativistic DWIA or a relativistic RDWIA are indeed able to give an excellent description of $(e, e'p)$ data [1, 2, 30–34].

In the inclusive scattering a model based on the DWIA or the RDWIA, where the cross section is given by the sum of all integrated one-nucleon knockout processes and FSI are described by a complex OP with an imaginary absorptive part, is conceptually wrong. The OP describes elastic nucleon-nucleus and its imaginary part accounts for the fact that, if other channels are open besides the elastic one, part of the incident flux is lost in the elastically scattered beam and goes to the inelastic channels which are open. In the exclusive reaction, where only one channel is considered, it is correct to account for the flux lost in the selected channel. In the inclusive scattering all the final-state channels are included, the flux lost in a channel must be recovered in the other channels, and in the sum over all the channels the flux can be redistributed but must be conserved. The DWIA and RDWIA do not conserve the flux.

Different relativistic approaches have been adopted, within the RIA, to describe FSI in the inclusive QE electron scattering. In the relativistic plane-wave impulse approximation (RPWIA) the plane-wave approximation is assumed for the emitted nucleon wave function and FSI are neglected. In other models FSI are incorporated in the emitted nucleon states by using real potentials, either retaining only the real part of the relativistic OP (rROP) or using the same relativistic energy-independent mean-field potential that describes the initial nucleon state (RMF) [17, 35–37]. Both the rROP and RMF conserve the flux, but the rROP is conceptually wrong because the optical potential has to be complex, owing to the presence of open inelastic channels. Its real and imaginary parts are related by dispersion relations and a model that arbitrarily omits a part is conceptually wrong. We note that the RMF fulfills the dispersion relations and maintains the continuity equation.

In the RGF model FSI are described in the inclusive scattering consistently with the exclusive scattering by the same complex ROP, but in the inclusive scattering the imaginary part conserves and redistributes the flux in all the channels. Detailed discussions of the model and of its formalism can be found, *e.g.*, in [12, 14, 16]. Here we summarize only the main steps.

With suitable approximations, which are essentially related to the RIA, the components of the hadron tensor can be written in terms of the single-particle (s.p.) optical model Green's function. The explicit calculation of the s.p. Green's function can be avoided exploiting its spectral representation, which is based on a biorthogonal expansion in terms of the eigenfunctions of the non-Hermitian ROP and of its Hermitian conjugate. The s.p. expression of the hadron-tensor components is then obtained in a form which contains matrix elements of the same type as the RDWIA ones of the exclusive $(e, e'p)$ process, but these matrix elements now involve eigenfunctions of the ROP and of its Hermitian conjugate, where the opposite sign of the imaginary part gives, in one case, an absorption and, in the other case, a gain of strength. Therefore, in the RGF model the imaginary part of the ROP redistributes the flux lost in the channel in the other (inelastic) channels and in the sum over all the channels the total flux is conserved. With the use of a complex ROP the model can recover the contribution of inelastic channels which are not included in other models based on the RIA: all the available final-state channels are included in the RGF and not only direct one-nucleon emission processes.

In the usual applications of the model the matrix elements are calculated using the same phenomenological bound and scattering states adopted in RDWIA calculations. We note that the use of a phenomenological ROP in the RGF calculations does not allow us to disentangle the contribution of a specific inelastic channel. Moreover, different parameterizations of the phenomenological ROP are available, which may provide equivalently good descriptions of elastic nucleon-nucleus scattering data, but which can give different results in RGF calculations and therefore introduce theoretical uncertainties in the numerical predictions of the model.

The results of different relativistic descriptions of FSI, in particular of the RGF and RMF, have been compared in [17]. The RGF and RMF results are always different from the results of the simpler RPWIA and rROP approaches. The differences between the RMF and RGF results increase with the momentum transfer. The differences of the RGF results obtained with different parameterizations of the ROP depend on kinematics and are basically due to the differences in the imaginary part of the ROPs. The real terms are very similar and the rROP cross sections are not sensitive to the parameterization used in the calculations.

The RGF provides in many cases a good description of the experimental (e, e') cross sections in the QE region, in particular in kinematic situations where the longitudinal response is dominant [14, 16–18].

In the case of charged-current QE (CCQE) (anti)neutrino-nucleus scattering the situation where only the final lepton is detected can be treated with the same models used for the inclusive QE (e, e') scattering. The RGF and RMF results have been compared in [22] for CCQE and in [27] for neutral-current elastic (NCE) scattering. Some differences are obtained with respect to the corresponding (e, e') results. The numerical differences between the RGF results for electron and neutrino scattering can mainly be ascribed to the combined effects of the weak current, in particular its axial term, and the imaginary part of the ROP [22]. The differences between the RGF and RMF results can be ascribed to the inelastic contributions which are incorporated in the RGF but not in the RMF (and in other models based on the RIA). The RGF and RMF give in many cases close predictions, usually different from those of the simpler RPWIA and rROP, but there are also kinematics situations where the differences are large [17, 22]. We recall that the RMF uses as input the real, strong, energy-independent, relativistic mean field potential that reproduces the saturation properties of nuclear matter and of the ground state of the nuclei involved. As such, it includes only purely nucleonic contribution and does not incorporate any information from scattering reactions. In contrast, the RGF uses as input complex phenomenological energy-dependent ROPs, which have been obtained through a fit to elastic proton-nucleus scattering data. Therefore, the RGF incorporates information from scattering reactions and takes into account all the allowed final states, as the s.p. Green's function contains the full propagator.

Since the imaginary part of the ROP includes the overall effect of the inelastic channels, we can expect that the differences between the RGF and RMF results increase with the relevance of such inelastic contributions. The comparison of the results of different models can therefore be useful to evaluate the relevance of inelastic contributions. In the comparison with data, we may expect that the RGF can give a better description of those experimental cross sections which receive significant contributions from non-nucleonic excitations and multi-nucleon processes. This is expected to be the case [23, 38] of MiniBooNE CCQE data.

The energy dependence of the ROP, which reflects the different contribution of the inelastic channels which are open at different energies, makes the RGF results very sensitive to the kinematic conditions of the calculations. Different kinematic conditions are generally considered in electron and neutrino scattering experiments. While in electron-scattering experiments the beam energy is known and the cross sections are given as a function of the energy transfer ω, in neutrino experiments ω and the momentum transfer q are not known, and the calculations for the comparison with data are carried out over the entire energy range which is relevant for the neutrino flux. The flux-average procedure can include contributions from different kinematic regions where the neutrino flux has significant strength and processes other than direct one-nucleon emission can be important. Part of these contributions are recovered in the RGF by the imaginary part of the ROP.

3 Comparison with CCQE and NCE Data

The first measurements of the CCQE flux-averaged double-differential $\nu_\mu(\bar{\nu_\mu})$ cross section on ^{12}C in the few GeV region by the MiniBooNE Collaboration have been reported in [4, 6]. The fact that the experimental cross sections are usually underestimated by models based on the RIA have suggested that effects beyond the RIA may play a significant role at MiniBooNE kinematics [38–43].

The results of different descriptions of FSI have been compared with the MiniBooNE data in [23, 24]. The RPWIA, rROP, and RMF generally underpredict the data, only the RGF gives larger cross sections, in reasonable agreement with the data, both for ν_μ and $\bar{\nu_\mu}$ scattering.

An example is presented in Figure 1, where the RGF double-differential ν_μ and $\bar{\nu_\mu}$ cross sections averaged over the MiniBooNE fluxes are displayed as a function of the muon kinetic energy T_μ for the $\cos\vartheta_\mu = 0.75$ angular bin. In the calculations the bound nucleon states are self-consistent Dirac-Hartree solutions derived within a relativistic mean-field approach [44]. The results of two differ-

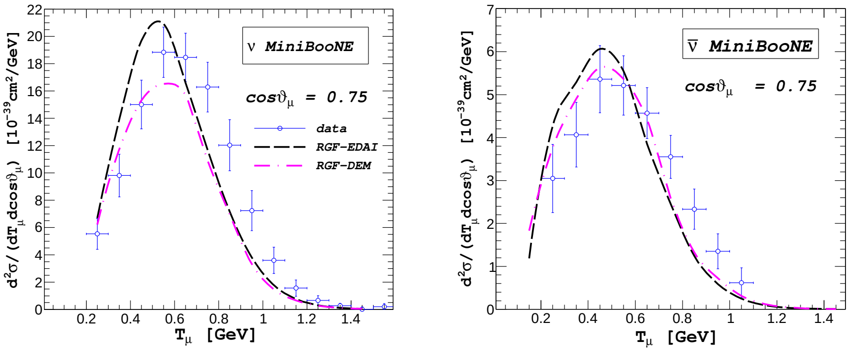

Figure 1. Flux-averaged double-differential cross section per target nucleon for the CCQE ^{12}C(ν_μ, μ^-) (left panel) and ^{12}C$(\bar\nu_\mu, \mu^+)$ (right panel) reactions as a function of the outgoing muon kinetic energy T_μ for the $\cos\vartheta_\mu = 0.75$ angular bin. calculated with the RGF-DEM and the RGF-EDAI. Experimental data from [4].

ent parameterizations of the ROP are compared: the energy-dependent and A-dependent democratic (DEM) [45] and the energy-dependent but A-independent EDAI [46]. While DEM is a global parameterization, which depends on the atomic number A and is obtained through a fit to more than 200 data sets of elastic proton-nucleus scattering data on a wide range of nuclei, EDAI is a single-nucleus parameterization, which is constructed to better reproduce the elastic proton-^{12}C phenomenology. In Figure 1 both RGF-DEM and RGF-EDAI are in reasonable agreement with the data around the peak region, while the data are slightly underpredicted for large T_μ.

The MINERνA Collaboration has recently measured differential cross sections for ν and $\bar\nu$ CCQE scattering on a hydrocarbon target [10, 11]. The experimental energy is higher than MiniBooNE. The RMF, which undepredicts the MiniBooNE data, provides a good description of the CCQE MINERνA data [47]. The RGF results give a satisfactory description of the MiniBooNE CCQE data and are very sensitive to the kinematic conditions of the calculations. In Figure 2 the RGF-EDAI and RGF-DEM differential flux averaged cross sections $d\sigma/dQ^2_{QE}$ for ν and $\bar\nu$ scattering off a CH target are displayed as a function of the reconstructed four-momentum transfer squared Q^2_{QE} and compared with the MINERνA data. Both RGF-EDAI and RGF-DEM are in good agreement with the data. The RGF-EDAI cross sections are, however, larger than the RGF-DEM ones for $Q^2_{QE} \lesssim 0.5$ GeV^2, while similar results are obtained with the two ROPs for larger values of Q^2_{QE}.

At MiniBooNE kinematics the RGF results are significantly larger than the RMF ones and in better agreement with the MiniBooNE data [23, 24]. The differences are reduced at MINERνA kinematics: the RGF results in Figure 2 are still somewhat larger than the RMF ones of [47] but in agreement with the data within the experimental errors.

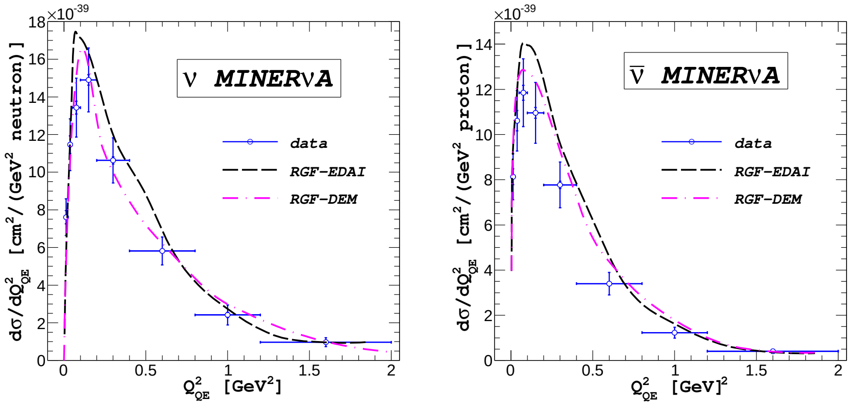

Figure 2. Flux-averaged differential $\nu-{}^{12}$C (left panel) and $\bar{\nu}-{}^{12}$C (right panel) cross section per target nucleon as a function of of Q^2_{QE} calculated with the RGF-DEM and the RGF-EDAI. Experimental data from [10, 11].

The MiniBooNE Collaboration has also measured NCE flux-averaged differential ν [5] and $\bar{\nu}$ [7] cross sections on CH_2 as a function of Q^2. The analysis of NCE reactions introduces additional complications, as the final neutrino cannot be measured and a final hadron has to be detected. Thus, NCE cross sections are usually semi-inclusive in the hadronic sector, where events for which at least one nucleon in the final state is detected are experimentally selected. The description of the semi-inclusive NCE scattering with the RGF can recover important contributions that are not present in the RDWIA, which is appropriate for the exclusive scattering but neglects some channels which can contribute to the semi-inclusive reaction. The RGF, however, describes the inclusive process and, as such, it may include channels which are not present in the semi-inclusive NCE measurements. From this point of view, the RDWIA can represent a lower limit and the RGF an upper limit to the NCE cross sections. In comparison with the MiniBooNE NCE data, the RDWIA generally underpredicts the experimental cross section, while the RGF results are in reasonable agreement with the NCE data [24].

In Figure 3, the RPWIA, rROP, and RGF $(\nu N \to \nu N)$ and $(\bar{\nu}N \to \bar{\nu}N)$ cross sections are displayed as a function of $Q^2 = 2m_N \sum_i T_i$. The variable Q^2 is defined assuming that the target nucleon is at rest, m_N being the nucleon mass and $\sum_i T_i$ the total kinetic energy of the outgoing nucleons. The RPWIA results, where FSI are neglected, show a satisfactory, although not perfect, agreement with the magnitude of the data whereas the rROP ones, which are calculated retaining only the real part of the EDAI potential, underestimate the data but for $Q^2 \geq 0.6$ (GeV$/c)^2$. The RMF cross sections in [27] are lower than the rROP ones and therefore below the data. Larger cross sections and a better agreement with the NCE data is provided by the RGF. The differences between RGF-DEM

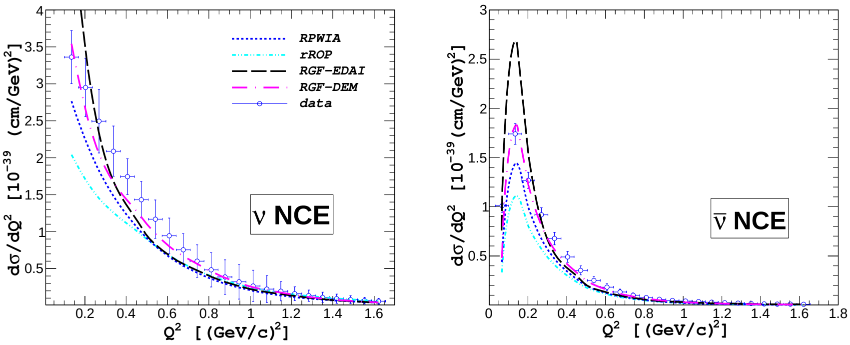

Figure 3. NCE flux-averaged differential $(\nu N \rightarrow \nu N)$ (left panel) and $(\bar{\nu} N \rightarrow \bar{\nu} N)$ (right panel) cross sections as a function of Q^2 calculated with the RPWIA, rROP, RGF-DEM, RGF-EDAD1, and the RGF-EDAI. Experimental data from [5, 7].

and RGF-EDAI calculations are due to the different imaginary parts of the two ROPs. The real parts are similar and give in practice the same rROP results. The best agreement with the data is provided by the RGF-DEM results.

In Figure 4, the ratio of the $\bar{\nu}$ to ν NCE cross sections are also presented. The MiniBooNE Collaboration performed both ν and $\bar{\nu}$ NCE measurements in the same beam line and with the same detector but with opposite horn polarities and, despite the fact that the experimental ν and $\bar{\nu}$ fluxes are not identical, the ratio of the two cross sections should minimize the errors and provide a useful observable to test various theoretical models. In Figure 4 all the models give very close results. In particular, the RGF results are practically independent of the parameterization adopted for the ROP. All the results are within the experimental errors, but for large Q^2, where they slightly underestimate the data.

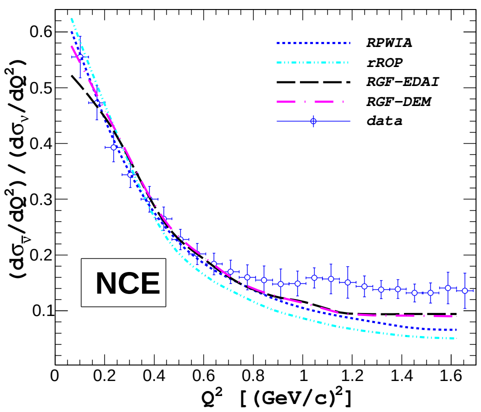

Figure 4. Ratio of the $\bar{\nu}$ to ν NCE scattering cross sections with total errors. Experimental data from [7].

4 Conclusions

We have reviewed some recent results of the RGF model. The model was developed to describe FSI in the inclusive QE electron scattering, it has been tested in comparison with electron-scattering data, and it has then been extended to QE neutrino scattering.

The RGF results are usually larger than the results of other models based on the RIA and are able to describe the CCQE MiniBooNE and MINERνA data and the NCE MiniBooNE data, both for ν and $\bar{\nu}$ scattering.

The RGF model is based on the use of a complex energy-dependent ROP whose imaginary part includes the overall effect of the inelastic channels, which give different contributions at different energies and make the RGF results sensitive to the kinematic conditions of the calculations. The use of the complex ROP allows us to include all the available final-state channels and not only direct one-nucleon emission processes. The important role of contributions other than direct one-nucleon emission has been confirmed by different and independent models in the case of MiniBooNE cross sections, but the same conclusion is doubtful in the case of the MINERνA data.

The RGF does not include two-body currents, but it can include rescattering processes, non-nucleonic Δ excitations, and also some multinucleon processes. Although not incorporated explicitly in the model, part of these contributions can be recovered, to some extent, by the imaginary part of the ROP. With the use of phenomenological ROPs, however, we cannot disentangle different reaction processes and explain in detail the origin of the enhancement.

The numerical predictions of the RGF are affected by the theoretical uncertainties in the determination of the phenomenological ROP. A better determination which closely fulfills the dispersion relations deserves further investigation.

References

[1] S. Boffi, C. Giusti, and F.D. Pacati, *Phys. Rep.* **226** (1993) 1-101.

[2] S. Boffi, C. Giusti, F.D. Pacati, and M. Radici, "*Electromagnetic Response of Atomic Nuclei*" Oxford Studies in Nuclear Physics, Vol. 20 (Clarendon Press, Oxford, 1996).

[3] O. Benhar, D. Day, and I. Sick, *Rev. Mod. Phys.* **80** (2008) 189-224.

[4] A.A. Aguilar-Arevalo *et al.*, *Phys. Rev. D* **81** (2010) 092005-1-22.

[5] A.A. Aguilar-Arevalo *et al.*, *Phys. Rev. D* **82** (2010) 092005-1-16.

[6] A.A. Aguilar-Arevalo *et al.*, *Phys. Rev. D* **88** (2013) 032001-1-31.

[7] A.A. Aguilar-Arevalo *et al.*, *arXiv:1309.7257*

[8] Y. Nakajima *et al.*, *Phys. Rev. D* **83** (2011) 012005-1-21.

[9] C. Anderson *et al.*, *Phys. Rev. Lett.* **108** (2012) 161802-1-5.

[10] L. Fields *et al.*, *Phys. Rev. Lett.* **111** (2013) 022501-1-7.

[11] G. Fiorentini *et al.*, *Phys. Rev. Lett.* **111** (2013) 022502-1-4.

[12] F. Capuzzi, C. Giusti, and F.D. Pacati *Nucl. Phys. A* **524** (1991) 681-705.

[13] F. Capuzzi *et al.*, *Ann. Phys.* **317** (2005) 492-529.
[14] A. Meucci *et al.*, *Phys. Rev. C* **67** (2003) 054601-1-12.
[15] A. Meucci, C. Giusti, and F.D. Pacati *Nucl. Phys. A* **756** (2005) 359-381.
[16] A. Meucci *et al.*, *Phys. Rev. C* **87** (2013) 054620-1-14.
[17] A. Meucci *et al.*, *Phys. Rev. C* **80** (2009) 024605-1-12.
[18] C. Giusti, A. Meucci, "*Nuclear Theory*" **32**, eds. A.I. Georgieva and N. Minkov (Heron Press, Sofia, 2013) pp. 50-60.
[19] A. Meucci, C. Giusti, and F.D. Pacati, *Nucl. Phys. A* **739** (2004) 277-290.
[20] A. Meucci, C. Giusti, and F.D. Pacati, *Acta Phys. Polon. B* **37** (2006) 2279-2286.
[21] A. Meucci, C. Giusti, and F.D. Pacati, *Acta Phys. Polon. B* **40** (2009) 2579-2584.
[22] A. Meucci *et al.*, *Phys. Rev. C* **83** (2011) 064614-1-10.
[23] A. Meucci *et al.*, *Phys. Rev. Lett.* **107** (2011) 172501-1-5.
[24] A. Meucci, C. Giusti, and F.D. Pacati, *Phys. Rev. D* **84** (2011) 113003-1-8.
[25] A. Meucci, and C. Giusti, *Phys. Rev. D* **85** (2012) 093002-1-6.
[26] A. Meucci, C. Giusti, and M. Vorabbi, *Phys. Rev. D* **88** (2013) 013006-1-7.
[27] R. González-Jiménez *et al.*, *Phys. Rev. C* **88** (2013) 025502-1-10.
[28] A. Meucci, and C. Giusti, *Phys. Rev. D* **89** (2014) 057302-1-4.
[29] A. Meucci, and C. Giusti, *Phys. Rev. D* **88** (2014) 117301-1-5.
[30] J.M. Udías *et al.*, *Phys. Rev. C* **48** (1993) 2731-2739.
[31] A. Meucci, C. Giusti, and F.D. Pacati, *Phys. Rev.C* **64** (2001) 014604-1-10.
[32] A. Meucci, C. Giusti, and F.D. Pacati, *Phys. Rev.C* **64** (2001) 064615-1-8.
[33] M. Radici, A. Meucci, and W.H. Dickhoff, *Eur. Phys. J. A* **17** (2003) 65-69.
[34] C. Giusti *et al.*, *Phys. Rev.C* **84** (2011) 024615-1-12.
[35] C. Maieron *et al.*, *Phys. Rev. C* **68** (2003) 048501-1-4.
[36] J.A. Caballero *et al.*, *Phys. Rev. Lett.* **95** (2005) 252502-1-4.
[37] J.A. Caballero, *Phys. Rev. C* **74** (2006) 015502-1-12.
[38] T. Leitner and U. Mosel, *Phys. Rev. C* **81** (2010) 064614-1-10.
[39] T. Leitner *et al.*, *Phys. Rev. C* **79** (2009) 034601-1-26.
[40] M. Martini *et al.*, *Phys. Rev. C* **80** (2009) 065501-1-16; *Phys. Rev. C* **81** (2010) 045502-1-5; *Phys. Rev. C* **84** (2011) 055502-1-7; *Phys. Rev. C* **87** (2013) 065501-1-5.
[41] A. Ankowski and O. Benhar, *Phys. Rev. C* **83** (2011) 054616-1-5.
[42] E. Fernandez Martinez and D. Meloni, *Phys. Lett. B* **697** (2011) 477-481.
[43] J. Nieves, I. Ruiz Simo, and M.J. Vicente Vacas, *Phys. Rev. C* **83** (2011) 045501-1-19; *Phys. Lett. B* **707** (2012) 72-75; *Phys. Lett. B* **721** (2013) 90-93.
[44] B.D. Serot and J.D. Walecka, *Adv. Nucl. Phys.* **16** (1984) 1-327.
[45] E.D. Cooper *et al.*, *Phys. Rev.C* **80** (2009) 034605-1-5.
[46] E.D. Cooper *et al.*, *Phys. Rev.C* **47** (1993) 297-311.
[47] G.D. Megias *et al.*, *Phys. Rev.D* **89** (2014) 093002-1.